

Supplementary Information for:

Ultra-high Output Charge Density Achieved by Charge Trapping Failure of Dielectric Polymers

Huiyuan Wu^a, Jian Wang^a, Wencong He^a, Chuncai Shan^a, Shaoke Fu^a, Gui Li^a, Qionghua Zhao^a, Wenlin Liu^{b*}, and Chenguo Hu^{a*}

^a Department of Applied Physics, Chongqing University, Chongqing 400044, P. R. China.

^b College of Chemistry and Molecular Engineering, Peking University, Beijing, 100871, P. R. China.

* Correspondence: liuwl-cnc@pku.edu.cn (W. Liu), hucg@cqu.edu.cn (C. Hu).

Key Words: charge excitation; charge density; output efficiency; charge trapping; carrier trap

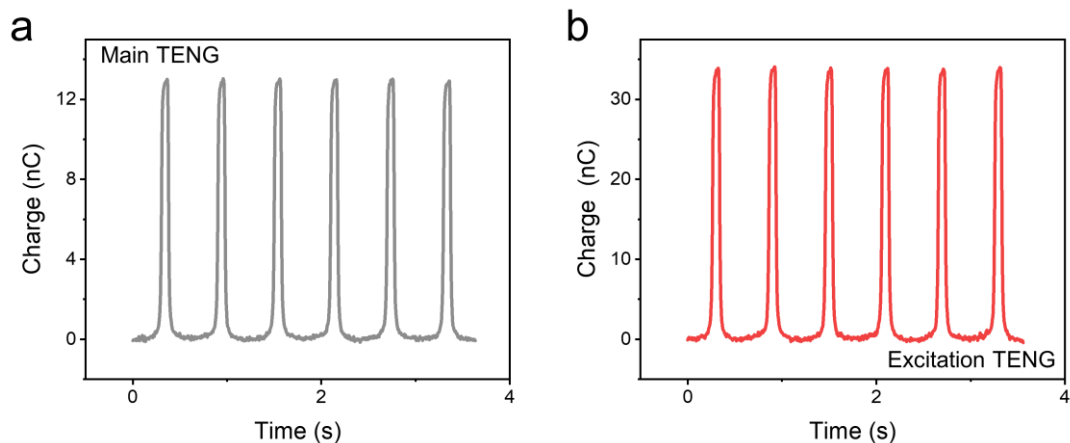


Figure S1. Output charge in independent measurement. (a) Output charge of the main TENG. (b) Output charge of the excitation TENG.

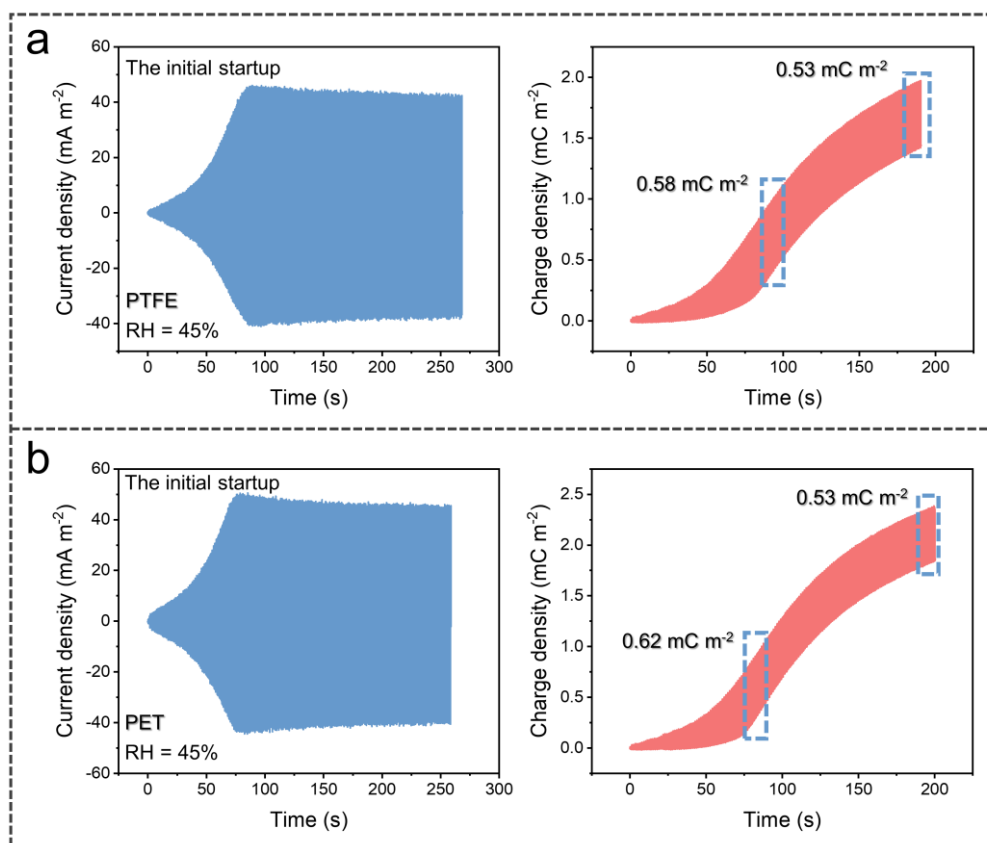


Figure S2. Dynamic output current density and output charge density when using different dielectric films in the initial startup of CE-TENG. (a) PTFE. (b) PET.

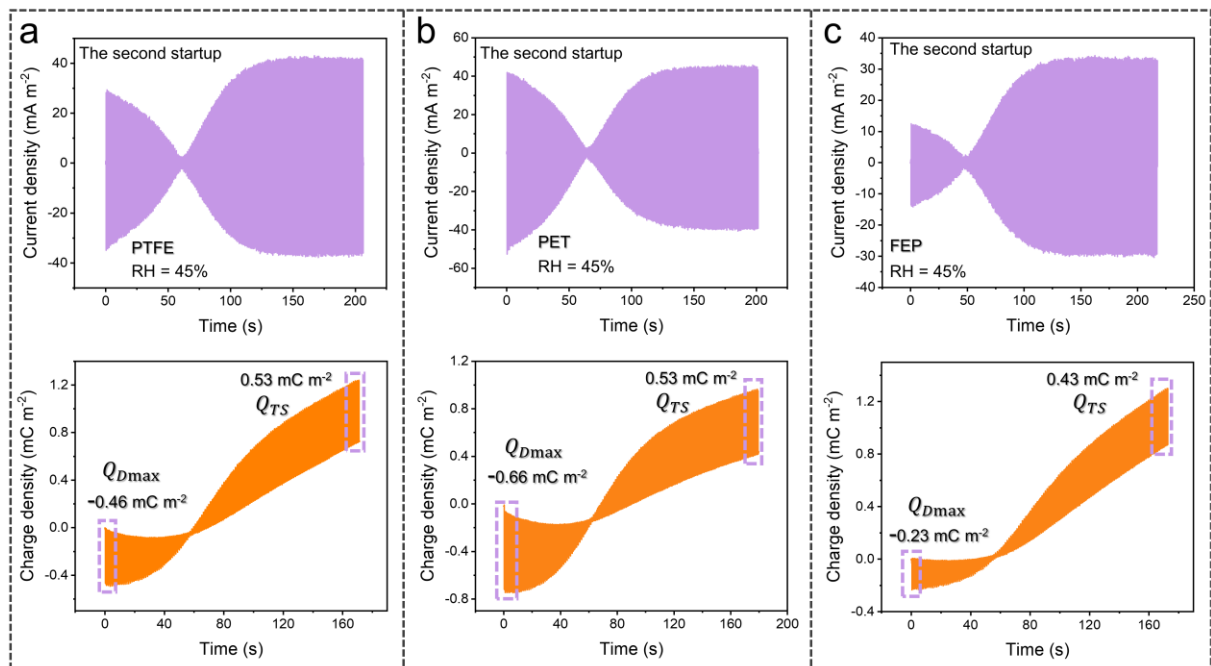


Figure S3. Dynamic output current density and output charge density when using different dielectric films in the second startup of CE-TENG. (a) PTFE (b) PET. (c) FEP.

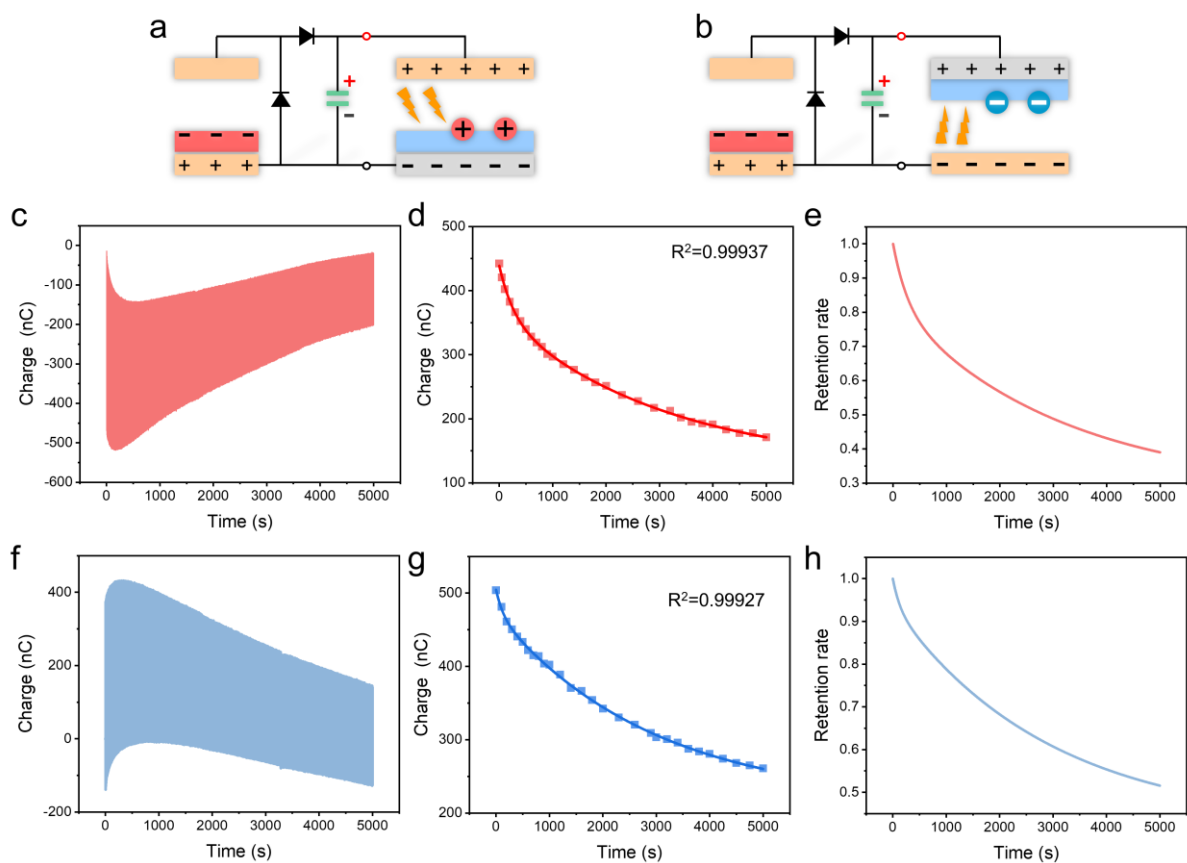


Figure S4. Characterization of trap states in dielectric films. (a) Schematic diagram of directional deposition of positive charge. (b) Schematic diagram of directional deposition of negative charge. (c) Output charge of positive deposition charge on PI film in 5000 s. (d) Fitting curve of positive deposition charge on PI film in 5000 s. (e) Normalization curve of positive deposition charge on PI film in 5000 s. (f) Output charge of negative deposition charge on PI film in 5000 s. (g) Fitting curve of negative deposition charge on PI film in 5000 s. (h) Normalization curve of negative deposition charge on PI film in 5000 s.

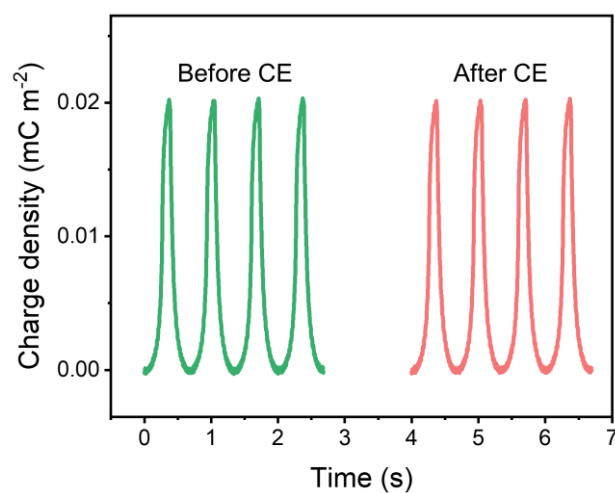


Figure S5. Output charge of PU film before and after charge excitation.

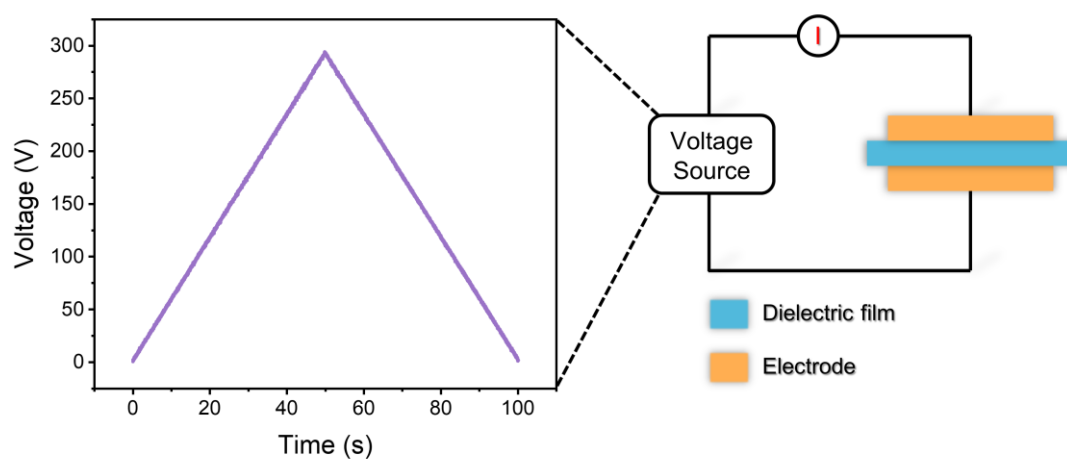


Figure S6. Test method of leak electricity characteristic.

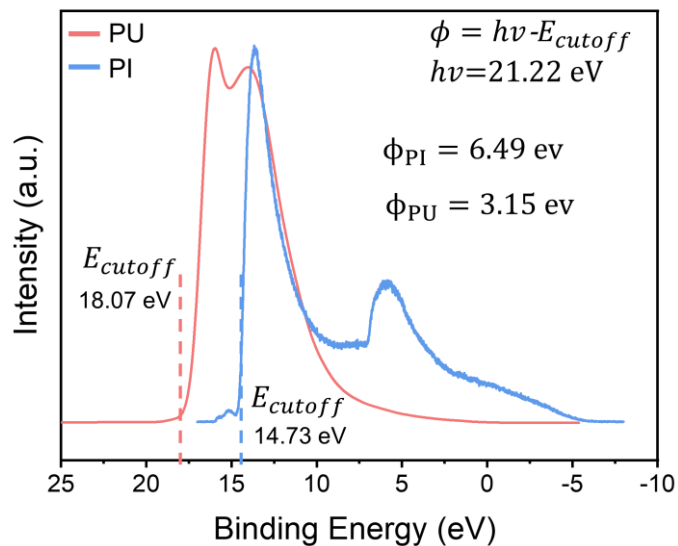


Figure S7. Work Function of PI and PU Films.

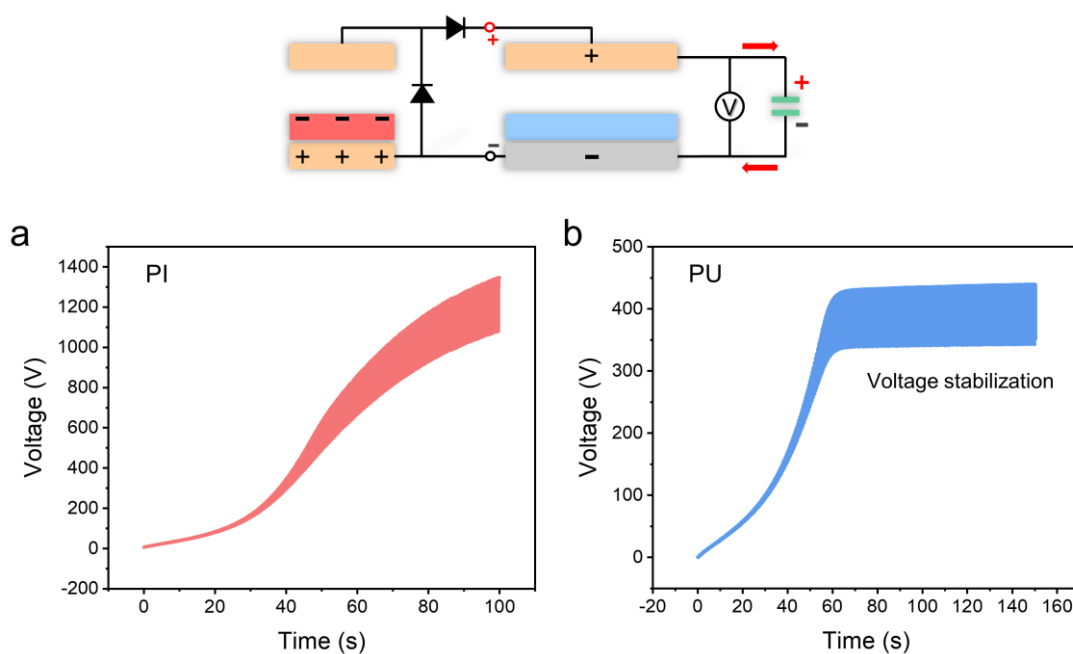


Figure S8. Variation process of the excitation voltage of (a) PI, and (b) PU films.

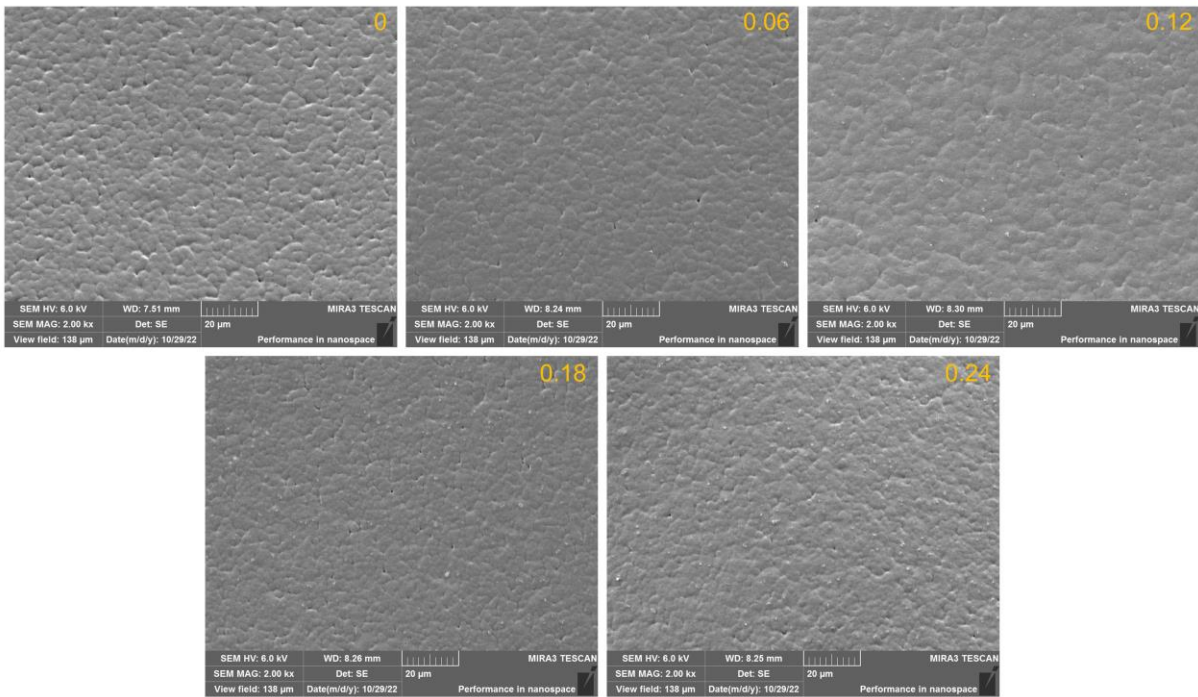


Figure S9. SEM images of CP-PVDF composite film with different filling concentrations (wt%).

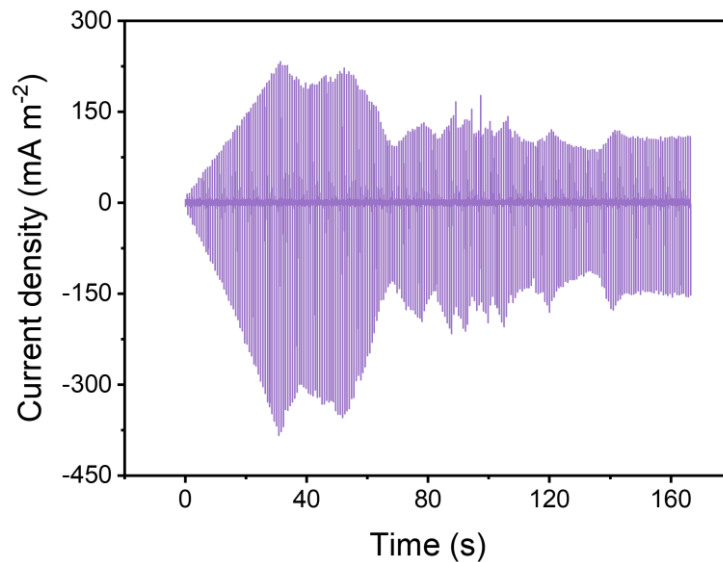


Figure S10. Dynamic output current density of the CP-PVDF composite film with filling concentration of 0.3 wt%.

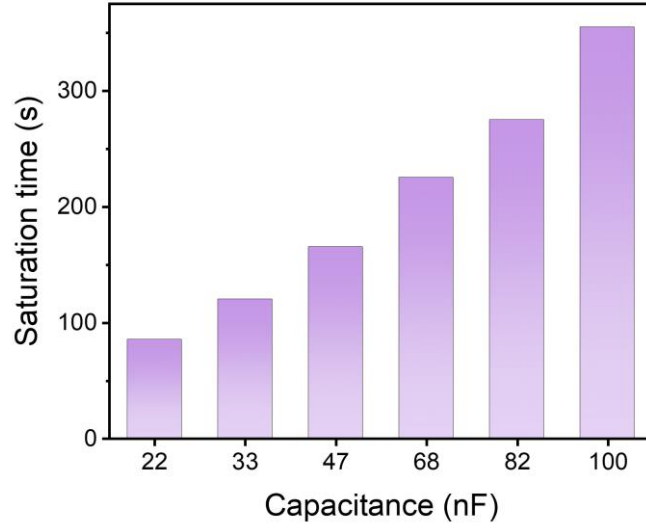


Figure S11. Output saturation time of CE-TENG under different external capacitances. CE-TENG can achieve rapid charge growth until it reaches a saturated state. The time required to reach the saturation state is defined as the saturation time of CE-TENG.

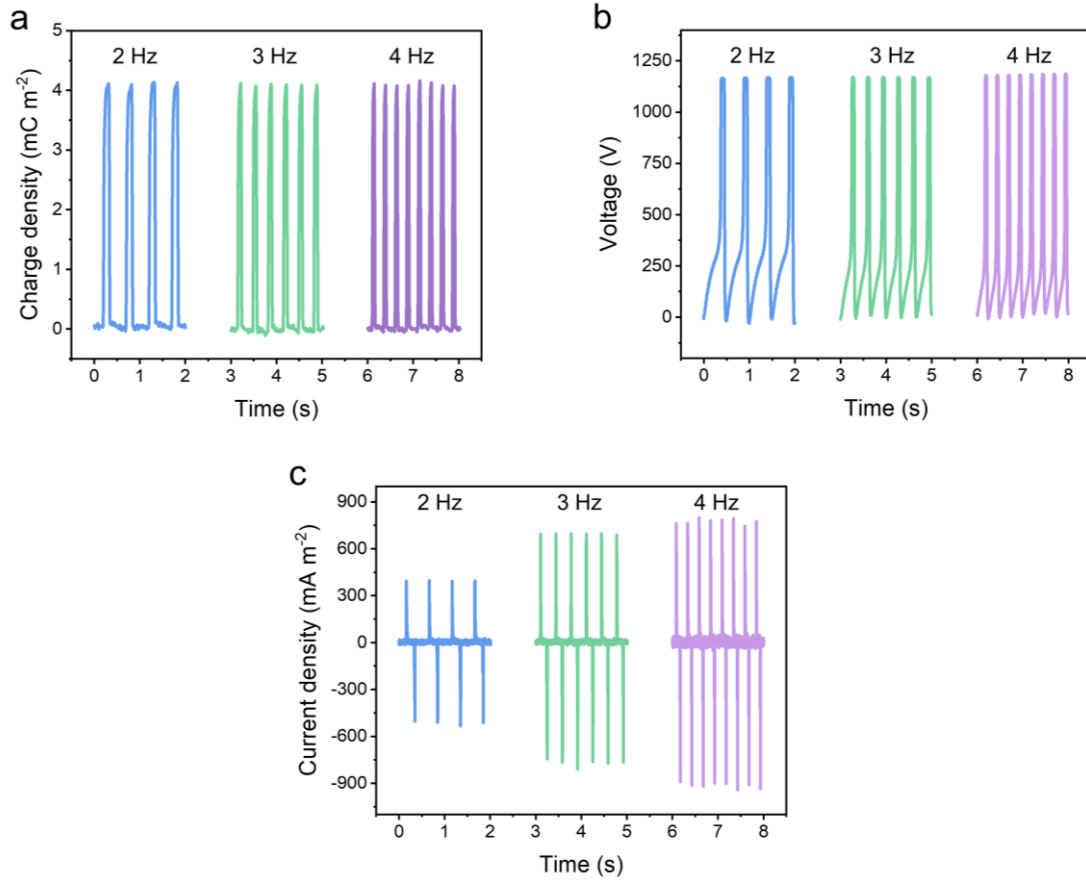


Figure S12. Output signal under various operation frequency. (a) Charge density. (b) Voltage. (c) Current density.

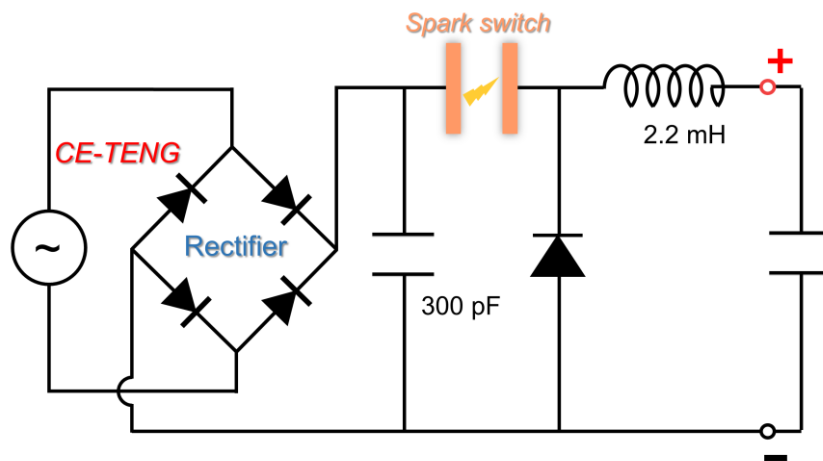


Figure S13. Circuit diagram of CE-TENG with an energy management unit for charging capacitor.

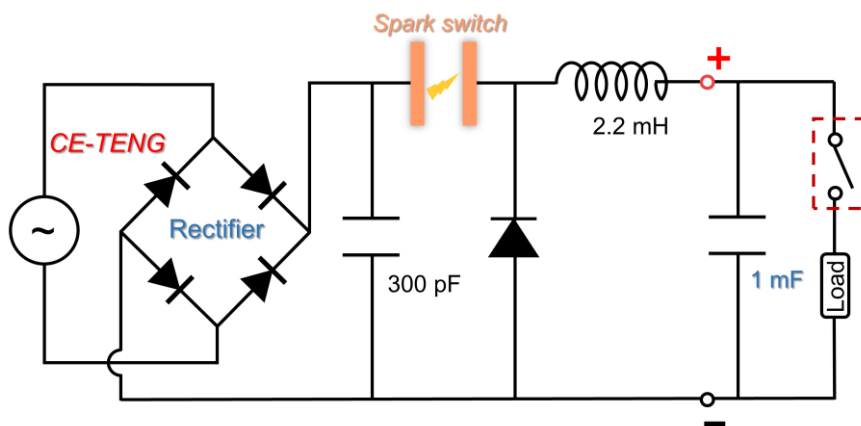


Figure S14. Circuit diagram of CE-TENG with an energy management unit for powering 4 hydrothermographs.

Note S1. Characterization of trap states of dielectric films.

As mentioned in the manuscript, the high excitation charge of CE-TENG can induce the occurrence of air breakdown, and the air ionized charge completes the directional deposition on the dielectric film under the traction of the excitation electric field. Particularly, we can change the direction of the excitation electric field to obtain positive deposition charge (**Fig. S4a**) and negative deposition charge (**Fig. S4b**). After sufficient charge deposition of CE-TENG, the main TENG is measured separately, in which the change of the output charge represents the change of the deposition charge. **Fig. S4c** shows the dynamic change process of positive deposition charge on PI film for 5000 s. In order to further obtain the decay curve of the deposition charge, the output charge values in **Fig. S4c** are selected at a certain time interval, and fit the selected points with the following equation (the result is shown in **Fig. S4d**):

$$Q(t) = ae^{-t/b} + ce^{-t/d} \quad (\text{S1})$$

where a, b, c, and d are the fitting parameters. Then, normalize the fitting curve, and the result is shown in **Fig. S4e**. Similarly, the attenuation information of the negative deposition charge is shown in **Fig. S4f-h**.

Trap state analysis method of dielectric materials (traps are the sites containing charges):

1. The attenuation information of positive and negative deposition charge corresponds to the state of hole traps and electron traps of dielectric material respectively.
2. The maximum deposition charge value (as the initial value in **Fig. S4d and g**) can reflect the total trap density of the dielectric film.
3. The retention rate of the deposition charge (as the curve in **Fig. S4e and h**) can reflect the trap energy level of the dielectric material. The lower the trap level is, the weaker the dielectric film's ability to retain the deposition charge is.

Based on the above information, we can make a preliminary judgment on the state of hole trap and electron trap of PI film. The maximum positive and negative charge that PI film (The area is 2.5 by 2.5 cm²) can accommodate are 438.9 nC and 504.6 nC respectively (**Fig. S4d and g**), which indicates that the electron trap density of PI film is larger than that of hole trap. The negative charge dissipates more slowly than the positive charge (**Fig. S4e and h**), which illustrates that the electron trap energy level of PI film is deeper.

Note S2. Calculation of trap parameters.

Isothermal surface potential decay (ISPD) method utilizes the surface potential decay curve $\varphi(t)$ of dielectric material to obtain specific trap parameters, including trap energy level and trap density, which was reported in detail by previous works^[1,2]. The surface potential of the dielectric film is proportional to the amount of surface charge. Therefore, in this work, we can assume that:

$$Q(t) = \varphi(t) \quad (\text{S2})$$

The trap density $N(E_T)$ of the dielectric material can be expressed as:

$$N(E_T) = \frac{\varepsilon_0 \varepsilon_r}{q_e f_0 K_B T L \delta} \left| t \frac{d\varphi(t)}{dt} \right| \quad (\text{S3})$$

where ε_0 is the vacuum permittivity (8.85×10^{-12} F m⁻¹), q_e is the unit charge (1.602×10^{-19} C), f_0 is the initial occupancy of the electron or hole (we set $f_0 = 1$). K_B is the Boltzmann constant (1.38×10^{-23} J K⁻¹). T is the ambient temperature. (we set $T = 300$ K). ε_r and L the relative permittivity and thickness of the dielectric material. δ is the range of an even charge distribution from the surface (we set $\delta = L$).

The trap level E_T of the dielectric material can be expressed as:

$$E_T = K_B T \ln(\gamma t) \quad (\text{S4})$$

where γ is the attempt-to-escape frequency of the trapped electrons (we set $\gamma = 2 \times 10^{13}$ s⁻¹).

Consequently, the trap parameters of dielectric material are obtained by combining the **Equation S3 and S4**. The specific parameters of deep traps and shallow traps can be obtained by dividing **Equation S1** into two items for calculation respectively.

Note S3. Measurement Method for KPFM.

Scheme: (refer to Fig. 4b and c)

Step 1: Place the dielectric film on the sample stage, and select a flat area to be measured (the size is 1 nm by 1 nm). Adjust the scanning frequency so that the scanning cycle of the probe from top to bottom is 800 s.

Step 2: Start measuring the surface potential of the selected area from top to bottom (0-70 s), and the measured value represents the initial potential of the dielectric film.

Step 3: At 70 s, apply a bias voltage of 5 V to the probe to achieve charge injection into the selected area.

Step 4: At 800 s, the probe completes scanning of the entire area. Immediately cancel the applied voltage to the probe.

Step 5: Immediately repeat the measurement of the surface potential of the selected area (800-1600 s), and the measured value represents the surface potential of the dielectric film after charge injection.

By comparing the data from Step 2 and Step 5, the charge trapping ability of the dielectric film can be evaluated.

Operating Steps

First, placed the sample in the area to be measured, and the sample is connected to the atomic force microscope sample stage with conductive adhesive. Then, set the potential module. Fix the probe about 50 nm above the sample. Set the Scan Size to 1nm, Scan Angle to 0 degree, and Scan Rate to 0.05 Hz. Next, open the Potential Channel, set the initial Simple Bias to 0 mV, and adjust the Simple Bias to 5000 mV after 70 s. When the scanning is over, remove the positive bias voltage and scan the sample again. All data are processed as raw data, and analyzed by Nano Scope Analysis software.

Table S1. The specific information of deposition charges, trap levels, and leakage currents of these materials.

Sample	Initial deposition charge (nC)	Deposition charge retention rate (After 5000 s)	Main trap level (eV)	Leakage current
PI	438.9	39%	1.001	5.6 nA
PTFE	403.4	73.7%	0.987	7.9 nA
PET	423.4	72.7%	1.005	3.9 nA
FEP	172.8	83.4%	0.982	9.9 nA
PVDF	635.8	4.6%	0.869	182.5 nA
PU	0	---	---	6.1 μA

Table S2. Output charge density comparison in the developmental stage of TENG.

Sample	Methods	Charge density (mC m ⁻²)	Reference
FEP-RRF	Repeated rheological forging	0.35	Nat. Commun., 2022, 13, 4083
PVDF/EP	Charge pumping	0.49	Nat. Commun., 2018, 9, 3773
PI	Charge injection	0.88	Adv. Funct. Mater., 2022, 32, 2203884
MXene/Silicone	Scalable surface modification	0.96	Adv. Funct. Mater., 2022, 32, 2107143
PTFE/BT	High vacuum	1.01	Nat. Commun., 2017, 8, 88
PI	Voltage-multiplying circuits	1.25	Nat. Commun., 2019, 10, 1426
PVC	High vacuum	1.25	Nat. Commun., 2022, 13, 6019
PVDF-BTO	Charge excitation	1.67	Adv. Funct. Mater., 2022, 32, 2204322
PP	Charge-shuttling	1.85	Nat. Commun., 2020, 11, 4203
PVDF-TrFE	High relative permittivity	2.20	Adv. Energy Mater., 2021, 11, 2100050
PEI	Improvement of contact efficiency	2.38	Nat. Commun., 2020, 11, 1599
PVDF-PZT	Self-polarization	3.53	Adv. Mater., 2022, 34, 2109918
PVDF-CP	Charge trapping failure	4.13	This work

Supplementary References

- 1 B. Zhang and G. Zhang, *J. Appl. Phys.*, 2017, **121**, 105105.
- 2 G. Chen and Z. Xu, *J. Appl. Phys.*, 2009, **106**, 123707.